DD

INSTITUTE FOR NUCLEAR STUDY
UNIVERSITY OF TOKYO
Tanashi, Tokyo 188
Japan

INS-Rep.-1069
Oct. 1994

The Superconducting Kaon Spectrometer – SKS –

T. Fukuda, T. Hasegawa, O. Hashimoto, A. Higashi, S. Homma, T. Kitami, Y. Matsuyama, T. Miyachi, T. Morimoto, T. Nagae, K. Omata, M. Sekimoto, T. Shibata
Institute for Nuclear Study, University of Tokyo, Tanashi, Tokyo 188, Japan

H. Sakaguchi, T. Takahashi
Department of Physics, Kyoto University, Kitashirakawa, Sakyo-ku, Kyoto 606-01, Japan

K. Aoki, Y. Doi, Y. Kondo, Y. Makida, M. Nomachi, H. Noumi, O. Sasaki, T. Shintomi
National Laboratory for High Energy Physics (KEK), Oho, Tsukuba, Ibaraki 305, Japan

H. Bhang, H. Park, M. Youn, H. Yu
Department of Physics, Seoul National University, Seoul 151-742, Korea

Y. Gavrilov
Institute for Nuclear Research, Academy of Science, 117312 Moscow, Russia

S. Ajimura, T. Kishimoto, A. Ohkusu, N. Shinkai
Department of Physics, Osaka University, Toyonaka, Osaka 660, Japan

K. Maeda
Department of Physics, Tohoku University, Kawauchi, Sendai, Miyagi 980-77, Japan

R. Sawafta
Physics Department, Brookhaven National Laboratory, Upton, NY 11973, USA

Submitted to Nucl. Instr. Meth. A

The Superconducting Kaon Spectrometer – SKS –

T. Fukuda, T. Hasegawa, O. Hashimoto, A. Higashi, S. Homma, T. Kitami, Y. Matsuyama, T. Miyachi, T. Morimoto, T. Nagae, K. Omata, M. Sekimoto, T. Shibata
Institute for Nuclear Study, University of Tokyo, Tanashi, Tokyo 188, Japan

H. Sakaguchi, T. Takahashi
Department of Physics, Kyoto University, Kitashirakawa, Sakyo-ku, Kyoto 606-01, Japan

K. Aoki, Y. Doi, Y. Kondo, Y. Makida, M. Nomachi, H. Noumi, O. Sasaki, T. Shintomi
National Laboratory for High Energy Physics (KEK), Oho, Tsukuba, Ibaraki 305, Japan

H. Bhang, H. Park, M. Youn, H. Yu
Department of Physics, Seoul National University, Seoul 151-742, Korea

Y. Gavrilov
Institute for Nuclear Research, Academy of Science, 117312 Moscow, Russia

S. Ajimura, T. Kishimoto, A. Ohkusu, N. Shinkai
Department of Physics, Osaka University, Toyonaka, Osaka 660, Japan

K. Maeda
Department of Physics, Tohoku University, Kawauchi, Sendai, Miyagi 980-77, Japan

R. Sawafta
Physics Department, Brookhaven National Laboratory, Upton, NY 11973, USA

A superconducting kaon spectrometer has been installed in the north experimental hall of the KEK 12-GeV proton synchrotron. The spectrometer was designed to serve for nuclear physics experiments with meson beams in the 1 GeV/c region, particular emphasis being laid on study of Λ-hypernuclei via (π^+,K^+) reactions. In order to obtain Λ-hypernuclear data with better statistics and energy resolution, it was designed to have a good momentum resolution of 0.1% FWHM and a large acceptance of 100 msr. It consists of a large superconducting dipole magnet, tracking chambers, and trigger counters that can efficiently select kaons from large background of pions and protons. The overall energy resolution for scattering is realized together with a beam-line spectrometer in the K6 beam line, the momentum resolution of which was also designed to be better than 0.1% FWHM. A good energy resolution of better than 2 MeV FWHM has been confirmed in π^--^{12}C elastic scattering and in the (π^+,K^+) reaction on ^{12}C.

1 Introduction

A new superconducting kaon spectrometer(SKS) has been installed in the KEK 12-GeV proton synchrotron(PS) and started operating in the beginning of 1992. The spectrometer is located at the newly constructed K6 beam line in the north experimental hall(N-Hall), where separated secondary beams in the momentum region around 1 GeV/c are delivered. While the primary purpose of the spectrometer is to study Λ-hypernuclei via (π^+,K^+) reactions, it is expected to be a general-purpose spectrometer which can serve nuclear physics experiments with secondary beams in the 1 GeV/c momentum region [1]. The understanding of hypernuclear structure has been so far limited by an available energy resolution (2.5∼5 MeV) and poor statistics. Therefore, the spectrometer was designed to have a good momentum resolution of 0.1% FWHM and to simultaneously achieve a large solid angle of 100 msr [2]. Since the momentum acceptance of the K6 beam line is wide(±3%), a beam-line spectrometer has been installed to measure the incident-particle momenta with a momentum resolution better than 0.1% FWHM. In the reaction spectrum with a target of reasonable thickness, our immediate goal has been to obtain a resolution of 2 MeV.

2 Design principle

2.1 K6 beam line

In the N-Hall, we presently have two beam lines, K5 and K6. The production target of the K6 beam line is located downstream of the same primary beam line. Usually, a platinum target having a size of 6ϕ×60 mm^2 is used as a production target. Figure 1 shows a schematic view of the K6 beam-line structure.

This beam line has been designed to serve mainly separated pions and kaons in

the momentum range between 0.5 and 2 GeV/c. For pions, we need both intensity and a good momentum resolution as in (π^+,K^+) reactions, while for kaons a good K/π separation with moderate intensity is required. In the old experimental hall at the 12-GeV PS, we have a similar beam line, K2. Compared with K2, there have been two modifications in K6 to improve the performance:

1. To realize a momentum resolution of 0.1% FWHM, the last portion of K6(QQDQQ) is used as a beam-line spectrometer by installing four sets of high-rate drift chambers(BDC1-4).

2. To remove any contamination due to decay pions around the production target, a vertical slit has been installed at the first vertical focusing point downstream of D1-Q1-Q2, which is expected to enhance the K/π ratio up to ~1.

The beam-line spectrometer has a dipole magnet with a bending angle of 60 degrees. It has been tuned to minimize the $\langle x|\theta\rangle$ term of its transfer matrix, so as to reduce the effect of multiple scattering in the chambers on the momentum resolution. The beam pipe in the QQDQQ system is evacuated with a Kapton window of 100 μm thickness. The transfer matrix of the beam-line spectrometer is calculated in the third order and is used for momentum reconstruction.

In Table 1, the design specifications of the K6 beam line are summarized.

2.2 The SKS Spectrometer

The design characteristics of the SKS spectrometer are summarized in Table 2. A good momentum resolution of 0.1% FWHM is one of the most important characteristics of the spectrometer for various forms of nuclear spectroscopy in the 1 GeV/c region. A superconducting magnet with a maximum field strength of 3 T ensures

a bending angle of 100 degrees up to ~1.1 GeV/c, which is vital for the required resolution. Since the momentum is obtained by measuring the particle trajectory, we need to minimize the total radiation length along the trajectory in order to avoid the effect of multiple scattering and to measure the magnetic-field distribution very precisely.

To obtain sufficient statistics, a large solid angle of 100 msr is required, which will enable us to efficiently carry out not only scattering experiments which measure very small cross sections($\leq$1 μb/sr), but also coincidence experiments for measuring weak decay particles emitted from hypernuclei, etc. This solid angle is almost one order of magnitude larger than those of spectrometers so far used for hypernuclear spectroscopy at CERN, BNL, and KEK. Since the momentum acceptance of the SKS is quite wide($\pm$10%), a large portion of the excitation spectrum can be measured at one time.

About 65% of the kaons at ~720 MeV/c emitted from the (π^+,K^+) reaction at 1.06 GeV/c decay within 5 m. To minimize this loss of kaons, the length of the spectrometer is made as short as 5 m.

In order to have a large solid angle and a short flight path simultaneously, a single-dipole configuration has been selected (Fig. 2). It is also useful to make the dipole a sector type with a pole-face rotation angle of 30 degrees because of its vertical focusing power.

To measure wide-angular distributions, the spectrometer can be rotated around the experimental target from $-10°$ to $40°$ while keeping the superconducting magnet at liquid-helium temperature.

3 Superconducting magnet

In order to realize a large acceptance of 100 msr and a good momentum resolution of 0.1% FWHM, a superconducting magnet with a pole gap of 50 cm and a maximum magnetic field of 3 T has been constructed [3]. Since the stored energy is very large, it is essential to use a superconducting magnet so as to avoid requiring an enormous amount of electric power consumption. As shown in Fig. 3, a sector-type magnet with an iron yoke has been selected because of its relatively simple fabrication as a superconducting magnet. From the view point of magnetic-field homogeneity, a window-frame type would be better. However, an H-type iron yoke has been adopted, taking account of the simplicity of the electromagnetic forces on the superconducting coils.

The parameters of the SKS spectrometer magnet are summarized in Table 3.

Intensive magnetic-field calculations were carried out using two kinds of three-dimensional computer codes, a finite element method and an integration one, for cross checking, because the iron yoke is completely saturated at 3 T and complicated magnetic-field distributions are expected. The calculated field distributions agreed well within an acceptable accuracy. The thickness of the return yoke has been chosen so that the leakage flux near to the top yoke surface can be suppressed to less than 500 Gauss. The support structure of the coils was designed on the basis of calculations of the electromagnetic forces on the coils, while taking account of a possible displacement from the stable position. The calculated magnetic-field strength on the superconducting wires is also important to determine the structure of the conductors.

The superconducting coil is cooled by pool-boiling helium. To cool down the coil, a main refrigerator with a cooling power of 350 W at 4.5 K(using liquid N_2) or 78.5 ℓ/h(without liquid N_2) has been constructed by KEK [4]. It supplies single phase helium gas in the supercritical state through a transfer line to the magnet. Since the magnet is required to be rotatable around the target to measure the angular distributions, the transfer line has rotary couplings at three points. The magnet, itself, is equipped with four air lifters at the bottom, which enable the magnet to float at a height of ~1 cm.

The helium vessel has 80 K thermal shields and 20 K anchors, which are cooled by a small G-M cooler mounted on top of the magnet yoke [5]. The small refrigerator is to be operated maintenance-free for more than one year. It suppresses any temperature increase when the main refrigerator is isolated from the magnet in between the beam cycles and shortens the cooling time. From room temperature the cooling time is ~50 hours, while it is typically 35 hours after one week from stopping the main refrigerator.

A high-precision highly-stabilized DC power supply has been installed for the magnet. The output current is stabilized within 5×10^{-5}/h and 1×10^{-4}/(8 h). The long-term drift of the output current is monitored by measuring the magnetic field at the pole surface with an NMR probe.

In Fig. 4, an excitation curve of the superconducting magnet is shown. A maximum magnetic field of 3.08 T was obtained at 506 A.

4 Detector system

4.1 Beam-line spectrometer

As shown in Fig. 1, the detector system of the beam-line spectrometer comprises four sets of high-rate tracking chambers(BDC1-4), two beam hodoscopes(BH1,2) and a gas Čerenkov counter(GC). The specifications are summarized in Table. 4.

4.1.1 Tracking chambers

The high-rate drift chamber has a drift distance of 2.5 mm, so that it can handle a maximum counting rate of up to several$\times 10^6$/sec/plane with a position resolution of 200–300 μm. The read-out electronics of the preamplifier and amplifier/discriminator are equipped with two-stage pole-zero cancellation and one baseline restorer for a high-rate capability (Fig. 5). The sense wire is a gold-plated 12 μm tungsten wire and the field wire is a gold-plated 75 μm copper-beryllium wire. To reduce the total thickness of the chamber in radiation length, the cathode planes are made of 7.5 μm Kapton foils, both sides of which are coated with Al(1000 Å) and Cr(~25 Å). In each set of chambers, there are six anode planes ($xx'uu'vv'$); in the u's and v's, the sense wires have stereo angles of $\pm$15 degrees to measure the vertical coordinate(y). In each pair plane (xx', uu' and vv'), the sense-wire position is shifted by half a cell size of 2.5 mm so as to resolve any left/right ambiguity. The sensitive area of each chamber is 24[W]$\times$14[H] cm^2. A gas mixture of Ar:C_4H_{10}:Methylal=76:20:4 is used at atmospheric pressure.

4.1.2 Beam hodoscopes

We use two sets of beam hodoscopes to define the beam. BH1 is installed upstream of BDC1. It is segmented into seven pieces of 5 mm-thick plastic scintillators in order to reduce the single-counting rates, and are used as a start timing counter for time-of-flight(TOF) measurements. The effective total area is 19$\times$9 cm^2. BH2 is located 60 cm upstream of the experimental target to define the beam actually hitting the target. The size of the counter is 8[W]$\times$10[H]$\times$0.2[T] cm^3. By using TOF information between BH1 and BH2, protons(~10%) in the π^+ beam are rejected in the trigger level.

4.1.3 Gas Čerenkov counter

A gas Čerenkov counter filled with Freon-12 at 1.2 kgf/cm^{2}G has been installed upstream of BH1 to reject positrons in the π^+ beam. It is used in the fast trigger level with a good detection efficiency of $\geq$99.9%. The number of positrons rejected is typically 20% of the π^+ at 1 GeV/c.

4.2 SKS detector system

The SKS detector system comprises four sets of tracking chambers (SDC1-4), a wall of TOF counter arrays, two layers of silica aerogel Čerenkov counters, and a wall of lucite Čerenkov counter arrays (Fig. 2). The specifications are summarized in Table. 5. The 50 cm-gap magnet is of the sector-type and can be excited up to 3 T, the central trajectory at 1 GeV/c being deflected by 100 degrees. The acceptance of the SKS for the (π^+,K$^+$) reaction is shown in Fig. 6.

4.2.1 Tracking chambers

At the entrance of the superconducting magnet there are two sets of drift chambers (SDC1,2) with a high-rate capability, in which the drift-cell structure is the same as that of the BDC's, since beam particles pass through the chambers. The sensitive area of each chamber is 40$\times$20 cm^2 and 56$\times$20 cm^2, respectively, in order to cover a wide angular range of $\pm$15 degrees in the horizontal plane. The SDC1 has six planes ($xx'uu'vv'$) and the SDC2 has only four planes ($u'xx'u$) so as to reduce any multiple-scattering effect.

At the exit of the superconducting magnet, we also have two sets of drift chambers (SDC3,4). Since the counting rate here is not very high, the drift-cell size ($\pm$21mm) is larger in both chambers compared with that in the other chambers. SDC3 has only

one plane (x) so as to make it as thin as possible. The last chamber (SDC4) comprises two sets of chambers (x and y) with six anode planes; the drift cell structure is shown in Fig. 7. The left/right ambiguity of the drift direction is resolved in each cell with the sense wire staggered by $\pm$ 200 μm. The sense wire is a gold-plated 20 μm tungsten wire and the field wire is a gold-plated 80 μm aluminum wire. The effective area of these chambers is 1×1 m^2. The gas mixture used is Ar:C_2H_6=50:50 at atmospheric pressure.

All the remaining space along the particle trajectories in between SDC1 and SDC4 is filled with He bags having thin windows to reduce multiple scattering.

4.2.2 Time-of-flight counter

The TOF counter is placed just behind SDC4. The counter comprises 15 segments of a plastic scintillator(BC408) of 7×100×3 cm^3. Each scintillator is viewed by two 2"-phototubes(Hamamatsu H1949) at both ends. The TOF resolution is 160 psec(rms).

4.2.3 Silica aerogel Čerenkov counter

There are two layers of silica aerogel Čerenkov counters(AC1,2). The first plane (AC1) covers 140×120 cm^2 with 9 cm-thick silica aerogels; the second plane (AC2) covers 140×140 cm^2 with 12 cm-thick silica aerogels. The refractive index was chosen to be about 1.06 so that the velocity of pions is above the threshold while that of kaons is below the threshold at around 720 MeV/c. A light-diffusion box was designed based on various prototype tests and Monte-Carlo simulations so as to obtain uniform efficiency over a large area[6]. The final design is shown in Fig. 8; the reflector plane is covered with aluminized mylar sheets. At both ends of the light-diffusion box, 18(20) 5"-phototubes(Hamamatsu R1584 modified) are mounted for AC1(AC2) in total.

The number of photoelectrons in one layer is measured to be about 6 over whole sensitive area for 720 MeV/c pions for various horizontal incident positions(Fig. 8). This enables us to reduce pions at the 10^{-3} level with two layers.

4.2.4 Lucite Čerenkov counter

The lucite Čerenkov counter comprises 14 vertical segments of a lucite counter having 10×140×4 cm^3. A wave-length shifter of bis-MSB was mixed by 10 ppm in weight in the lucite radiator in order to enhance the detection efficiency for pions and kaons with various incident angles. The number of photons at the phototube has been increased by a factor of two. Protons slower than 850 MeV/c are mostly rejected because of the Čerenkov light threshold(the refractive index of lucite is 1.5); the sensitivity for 700 MeV/c protons is only 10%.

4.3 Data-taking system

A diagram of the SKS data-taking system is shown in Fig. 9.

Most of the signals from the detecters in the SKS and beam-line spectrometers are digitized with TDC and ADC modules in TKO boxes. The TKO is a standard developed at KEK [7]: 32-ch. TDC modules for the drift-chamber readout, 16-ch. high-resolution TDC modules, and 32-ch. charge ADC modules are used in the present setup. Those modules are stored in six TKO boxes.

In each box there is one controller module (TKO-SCH (Super Controller Head)), which has various scanning modes with pedestal subtraction, threshold cut, and clustering capabilities. The scanning sequence is triggered by a NIM signal supplied at the front panel of a VME module (VME-MP(Memory Partner)). The VME-MP is an interface module between the TKO TOWEL bus and the VME bus. For each trigger

signal, data are transferred(250 KBytes/sec/module) from TKO-SCH to VME-MP and stored in a local memory of 256 KBytes on the VME-MP.

The stored data are read out by a VME MC68020 CPU module during a beam-off period of 2.5 sec. every 4 sec. CAMAC scalers in one crate are also read out during this period via a VME-CAMAC interface (CES-8216) connected to a K3922 CAMAC crate controller. The CPU module works under the VME/OS9 system. A buffer management utility, "NOVA" [8], developed by the KEK online group, controls the data taking in this system. The data processed by NOVA are written on an 8-mm video tape via a SCSI interface, and are also transferred(0.7~1 Mbytes/sec) to a DEC Station 5000/200 via DRE68 [9] for online monitoring. The great CPU power in the workstation enables us to monitor the kaon yields and the momentum spectra with software track reconstructions in an online analysis. The data-taking efficiency is 92±1% for (π^+,K^+) reactions with a typical data size of 200 words/trigger and a trigger rate of ~400/spill; up to ~1000/spill is acceptable.

5 Performance

5.1 Pion beam

Typically, 2.5–3.0×10^{12} ppp is on the production target at K6 when K5 is also in operation. So far, the beam tuning for pions has been carried out so as to maximize the pion yield and to obtain reasonable focusing at the experimental target position. The maximum positive pion intensity obtained is 5.5×10^6 at 1 GeV/c for 2.5×10^{12} ppp. To keep the accidental hit rate and counter dead time sufficiently small, the intensity has been kept to be 3.0×10^6/spill on the target. A typical beam size at the target is 0.6[H]×0.7[V] cm^2(rms). The contamination of muons in the pion beam is estimated to be 6±2% based on an analysis using the computer code "Decay Turtle" [10].

5.2 Kaon trigger

The kaon trigger for the (π^+,K^+) reaction is generated according to the logic signal of $BH1 \cdot BH2 \cdot \overline{GC} \cdot TOF \cdot LC \cdot \overline{AC}$ (Fig. 10). Due to the high detection efficiency of the silica aerogel Čerenkov counter for pions, we could greatly suppress the trigger rate. The lucite Čerenkov counter also suppressed the triggers caused by low-momentum protons. As a result, the typical trigger rate for (π^+,K^+) reactions for 2 g/cm^2 targets is 400 triggers/spill at a pion intensity of 3.0×10^6/spill on the target, which could be handled by our data-taking system with high efficiency. The number of true (π^+,K^+) events is ~1 out of 400 triggers.

5.3 Particle identification

After track reconstruction in the SKS tracking system the scattered particles are identified based on the TOF between BH1 and the TOF counter correcting the flight-path length and momentum. A TOF resolution of 160 psec enables us to clearly identify kaons, as shown in Fig. 11, in which the mass distribution of the scattered particles is plotted for the ^{12}C(π^+,K^+) reaction.

5.4 Magnetic-field measurement

Since the error in the magnetic-field measurement directly affects the momentum resolution of the SKS, a measurement error on the order of 0.01% is required to obtain an overall momentum resolution of 0.1%. In order to realize this accuracy, there are two important points: one is for a good Hall probe to have such a precision; the other is to measure the position of the Hall probe with an accuracy of 500 μm(including systematic error) within the total measurement volume.

We selected a temperature-compensated Hall probe (DTM-141-S) supplied by GMW Group 3 [11], which has the specifications listed in Table 6. Since the magnetic-field gradient is so large, we chose a small sensitive area of 0.5×1.0 mm^2. The precision and stability was calibrated with an NMR probe in a uniform magnetic-field area. The Hall planar effect has influence at the 1% level of the magnetic field. The correction parameters were measured by using a device which has two rotating axes. The magnetic-field dependence of the parameters was also obtained. Three probes were mounted on a 2 cm cube in order to measure three components of the magnetic field. We used six probes in total.

The ambiguity of the Hall-probe position causes an error in the magnetic field because of a large field gradient near to the pole-piece edge. A fully-automated measuring system was constructed and mounted on the return yoke, as shown in Fig. 12. The moving three axes defined the Cartesian coordinate referred to the pole face having a point-by-point accuracy within 500 μm. The local precision in each axis was 25 μm with an optical scale. The relative position between the Hall probes and the magnet yoke was calibrated by measuring the local field caused by conical pins mounted on the pole-piece surface. The overall precision of the Hall probes is 500 μm in position and 3 mrad in inclination.

The magnetic-field distributions were measured at seven excitations (1.5, 1.72, 1.93, 2.22, 2.4, 2.65 and 3 T) which correspond to central momenta of 500, 570, 630, 720, 780, 860 and 970 MeV/c, respectively. In each excitation we measured the distribution at 1.2×10^5 points with 1–5 cm(mainly 2 cm) meshes, which covered the total tracking region.

The precision of the reconstructed magnetic fields was evaluated using three methods: the differences in the overlap regions, a comparison with the calculated magnetic field as the solution of a boundary-value problem, and an internal-consistency check as to whether the Poisson equation is satisfied locally. In the measurement, the total volume was divided into ten regions. Some overlap regions were measured independently. The agreement was quite good. The magnetic-field distribution can be calculated based on the magnetic fields at the surface of a volume as a solution of a boundary-value problem of Maxwell's equations [12]. The calculated field agreed with the measured field within a precision of $\pm 0.03\%$. The local consistency of the magnetic fields can also be examined by checking whether the local fields satisfy the Poisson equation, $\nabla \cdot \vec{B}=0$. The result is consistent with the required precision.

5.5 Momentum resolution

The momentum of a beam particle is obtained by using a calculated third-order beam-transfer matrix of the QQDQQ system and the momentum of a scattered particle in the SKS by the Runge-Kutta method [13] using the measured field maps. The momentum resolution of the spectrometer system was examined by letting a 720 MeV/c pion beam through the two spectrometers and by measuring the difference in the momenta determined by each spectrometer. The beam-transfer matrix of the beam-line spectrometer was optimized by correcting the obtained momentum with the SKS momentum. The resolutions of the beam-line and the SKS spectrometers were found to be 0.1% FWHM, respectively, after the correction (Fig. 13). From a Monte-Carlo simulation, the momentum resolution is mostly determined (0.7∼0.9 MeV/c FWHM) by the accuracy of the magnetic-field measurement, while the multiple scattering and the position resolution of the tracking chambers contribute at the 0.5∼0.6 MeV/c FWHM level.

5.6 Energy resolution

Examples of two (preliminary) reaction spectra are shown in Figs. 14 and 15. Figure 14 is an excitation spectrum of ^{12}C observed in the 800 MeV/c pion scattering on a thick ^{12}C target. A hypernuclear spectrum for the (π^+,K$^+$) reaction at 1.06 GeV/c on a 0.89 g/cm^2 ^{12}C target was obtained (Fig. 15), in which the spectrum is plotted against the negative of the Λ binding energy. Two large peaks corresponding to the s- and p- Λ orbitals in $^{12}_{\Lambda}$C can be seen. Two additional small peaks in between are clearly observed for the first time. In both spectra, an energy resolution of 2 MeV is achieved.

In order to obtain the 2 MeV resolution, it is important to monitor the long-term drift of the momentum in each spectrometer. First the central momentum was corrected by using the measured magnetic field at the pole face of each dipole magnet. The matching of two momenta for the pion beam was also calibrated once in a few days.

6 Summary

The superconducting kaon spectrometer (SKS) started operating in the beginning of 1992 at the KEK 12-GeV PS. It has been constructed as a general purpose spectrometer in the 1 GeV/c region with a large solid angle of 100 msr and a good momentum resolution of 0.1% FWHM. Together with the beam-line spectrometer in the K6 beam line, we have already confirmed that the spectrometer system has a momentum resolution of 0.1% FWHM, as designed. Even in preliminary analyses, good energy resolutions of better than 2 MeV have been obtained in the reaction spectra of ^{12}C(π^-,π^-) at 800 MeV/c and ^{12}C(π^+,K$^+$)$^{12}_{\Lambda}$C, which should be very useful for various future experiments. So far, three experiments have completed their data

taking: one is an experiment(E269) measuring pion elastic and inelastic scattering on a ^{12}C target at five incident momenta from 0.624 GeV/c to 1 GeV/c; the second is an experiment(E140a) measuring heavy hypernuclear spectra up to ^{208}Pb by the (π^+,K$^+$)reaction; the third is an experiment(E278) concerning the weak decay of polarized $^{5}_{\Lambda}$He. A new experiment involving lifetime measurements of Λ hypernuclei is being prepared.

Acknowledgments

We are grateful for the continuous support by Professor T. Yamazaki of INS and by Professors H. Hirabayashi and K. Nakai of KEK through the construction and installation of the SKS. For the design, construction and commissioning of the K6 beam line, we would like to thank Dr.M. Ieiri of the KEK-PS beam-channel group. We wish to acknowledge Drs.S. Toyama, M. Torikoshi, Y. Kawashima and I. Nomura for the design and prototype tests of the silica aerogel Čerenkov counter etc. For the design of the superconducting magnet, particularly the 3-dimensional magnetic field calculations, we would like to thank Mr.Y. Yamanoi of KEK. We also thank Prof.S. Kato of Yamagata University for valuable discussions concerning the spectrometer design and Prof.J. Imazato of KEK for critical suggestions regarding the design of the refrigerator system. We are also indebted to Professors Y. Shida and F. Soga for their contribution at the designing stage of the spectrometer.

References

[1] O. Hashimoto, in Perspectives of MESON SCIENCE, eds. T .Yamazaki, K. Nakai and K. Nagamine (North-Holland, Amsterdam, 1992) p547.

[2] O. Hashimoto *et al.*, *Il Nuovo Cimento* **102** (1989) 679.

[3] T. Shintomi *et al.*, *IEEE Trans. on Magnetics*, **MAG-25** (1989) 1667, T. Shintomi *et al.*, *IEEE Trans. on Magnetics*, **MAG-28** (1992) 585.

[4] K. Aoki *et al.*, *Advance in Cryogenic Engineering* **37** (1992) 691.

[5] T. Kitami *et al.*, INS Technical report, INS-T-517 (1993).

[6] T. Hasegawa *et al.*, *Nucl. Instr. Meth. A* **342** (1994) 383.

[7] T.K. Ohska *et al.*, KEK Report, 85-10 (1985).

[8] M. Nomachi, private communications.

[9] Y. Yasu *et al.*, Proc. Computing in High Energy Physics '91, eds. Y. Watase and F. Abe (Universal Academy Press, Tokyo, 1991) p653.

[10] K.L. Brown *et al.*, CERN 74-2 (1974).

[11] Group 3 Technology Ltd., 2 Charann Place, Avondale, Auckland 7, New Zealand, P.O. Box 71-11.

[12] H. Wind, *Nucl. Instr. Meth.* **84** (1970) 117.

[13] J. Myrheim *et al.*, *Nucl. Instr. Meth.* **160** (1979) 43.

Momentum range	0.5~2.0 GeV/c
Momentum bite	±3%
Momentum resolution	0.1% FWHM
Acceptance	1.9 msr
Typical intensity	6.5×10^{6} π^{+}
for 10^{12} protons/pulse	3.3×10^{3} K^{-}
	(at 1 GeV/c)
Channel length	30 m

Table 1: Design specifications of the K6 beam line.

Momentum resolution	0.1% FWHM at 720 MeV/c
Maximum central momentum	1.1 GeV/c
Momentum bite	±10%
Bending angle	100° for the central trajectory
Solid angle	100 msr
Flight path	~5 m for the central trajectory

Table 2: Characteristics of the SKS spectrometer.

Maximum magnetic field	3 T
Maximum field on conductors	4.5 T
Stored Energy	10.6 MJ
Pole Gap	49.75 cm
Coil Cross Section	15×12 cm^2
Conductor	NbTi/Cu
Ampere Turns	2.1 MA·T
Maximum Current	500 A
Inductance	86.9 H
Cold Mass Coil	4.5 tons
Shield	0.44 tons
Weight of yoke	263 tons
Total Weight	280 tons
Heat Leak at 4K	5 W
Content of Liquid He	156 ℓ

Table 3: Parameters of the SKS spectrometer magnet.

Detector	Area (cm)	Drift space (mm)	Wires	Thickness (in L_R)
BDC1–4	24[W]×15[H]	2.5	$xx'uu'vv'$	1.79×10^{-3}

Detector	Area (cm)	PMT (Hamamatsu)	etc.
BH1	19×9×0.5	R1450×14	7 segments
BH2	8×10×0.2	H1161×2	1 segment
GC	20ϕ×29	R1584-02	Freon-12, n=1.00245

Table 4: Specifications of the beam-line detectors.

Detector	Area (cm)	Drift space (mm)	Wires	Thickness (in L_R)
SDC1	40[W]×20[H]	2.5	$xx'uu'vv'$	1.79×10^{-3}
SDC2	56[W]×20[H]	2.5	$u'xx'u$	1.18×10^{-3}
SDC3	100[W]×100[H]	21	x	0.53×10^{-3}
SDC4	100[W]×100[H]	21	x×6+y×6	2.1×10^{-3}

Detector	Area (cm)	PMT (Hamamatsu)	etc.
TOF	105×100×3	H1949×30	15 segments
AC1	140×120×9	R1584-02×18	n=1.06
AC2	140×140×12	R1584-02×20	n=1.06
LC	140×140×4	H1949×28	14 segments, n=1.5

Table 5: Specifications of the SKS detectors.

Sensitive Area	0.5×1.0 mm^2
Maximum Field	3 T
Resolution	5×10^{-5} T
Precision	0.02% at 25 $^{\circ}C$
Temperature Stability	$\pm$0.01%/$^{\circ}C$
Long-term Stability	$\pm$0.1%/year

Table 6: Specifications of the Hall probe GMW DTM-141-S.

Figure Captions

Fig. 1 Schematic floor plan of the K6 beam-line area in the north experimental hall of the 12-GeV KEK-PS.

Fig. 2 Schematic view of the SKS with typical particle trajectories.

Fig. 3 Schematic drawings of the SKS spectrometer magnet. The return yoke comprises 18 layers of iron plates.

Fig. 4 Excitation curve of the superconducting magnet.

Fig. 5 Schematic diagram of the preamplifier and the amplifier/discriminator module.

Fig. 6 Acceptance of the SKS spectrometer for the (π^+,K^+) reaction as a function of the particle momentum.

Fig. 7 Drift-cell structure of SDC4. There are six anode planes in each cell with focusing wires. The anode wires are staggered by $\pm200\mu$m.

Fig. 8 (a) Structure of the light diffusion box. (b) Position dependence of the number of photoelectrons obtained in one layer.

Fig. 9 Diagram of the SKS data-taking system.

Fig. 10 Logic diagram of the SKS for the (π^+,K^+) reaction.

Fig. 11 Mass distribution of the scattered particles based on TOF information and the momentum for the (π^+,K^+) reaction.

Fig. 12 Bird's-eye view of the volume-scanning device for the magnetic-field measurement.

Fig. 13 Difference in the momenta measured with the beam-line spectrometer and the SKS for a pion beam at 720 MeV/c. The width shows that the resolutions of the two spectrometers are 0.1%.

Fig. 14 Excitation spectrum of ^{12}C in the reaction of 800 MeV/c π^- + ^{12}C.

Fig. 15 Hypernuclear spectrum measured by the reaction $^{12}C(\pi^+,K^+)^{12}_{\Lambda}C$ at 1.06 GeV/c.

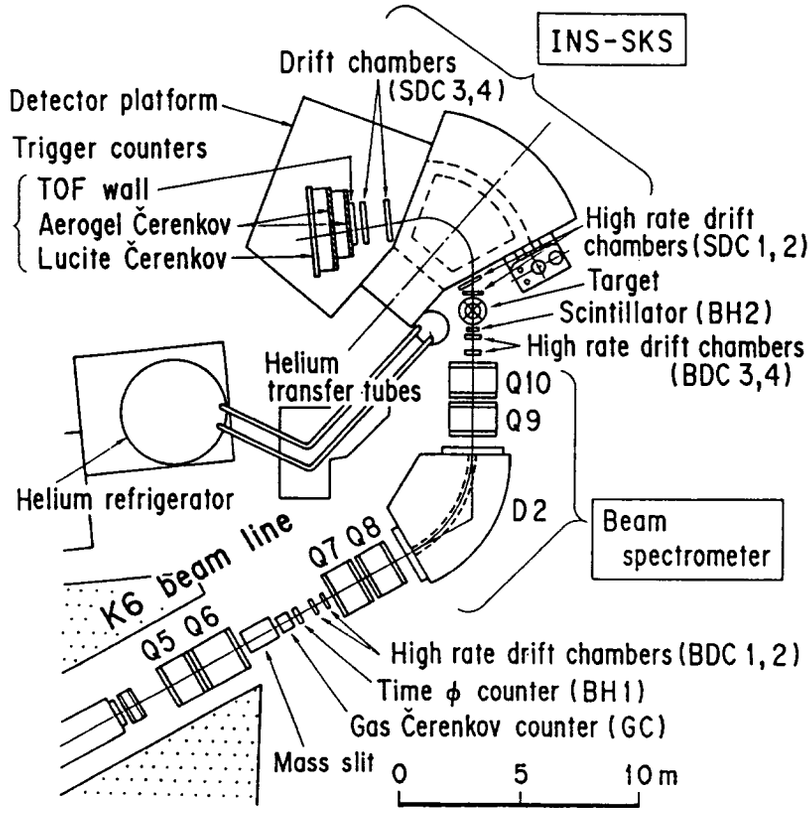

Figure 1: Schematic floor plan of the K6 beam-line area in the north experimental hall of the 12-GeV KEK-PS.

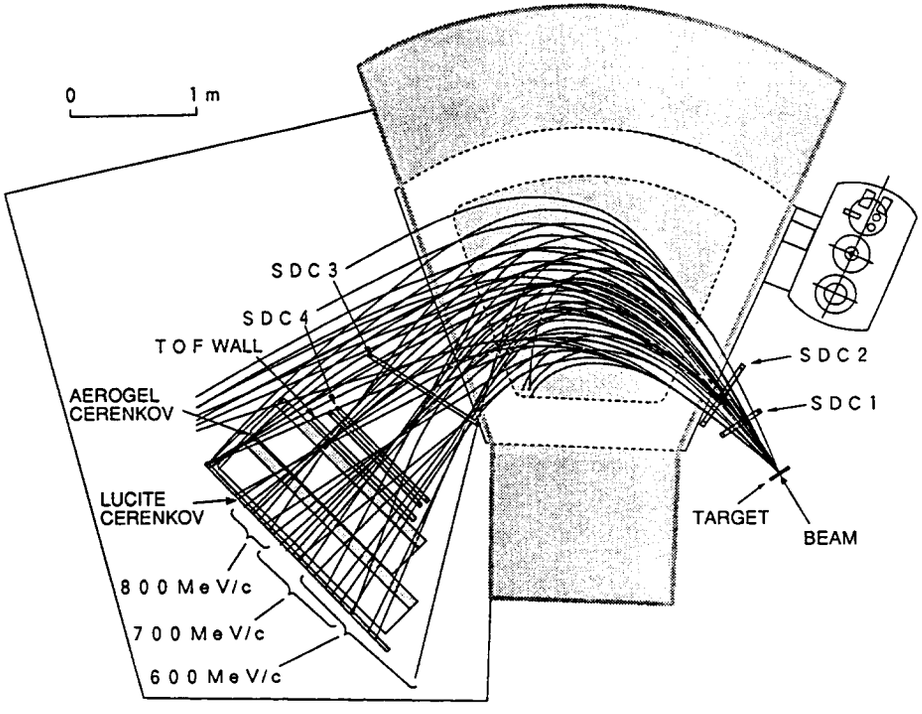

Figure 2: Schematic view of the SKS with typical particle trajectories.

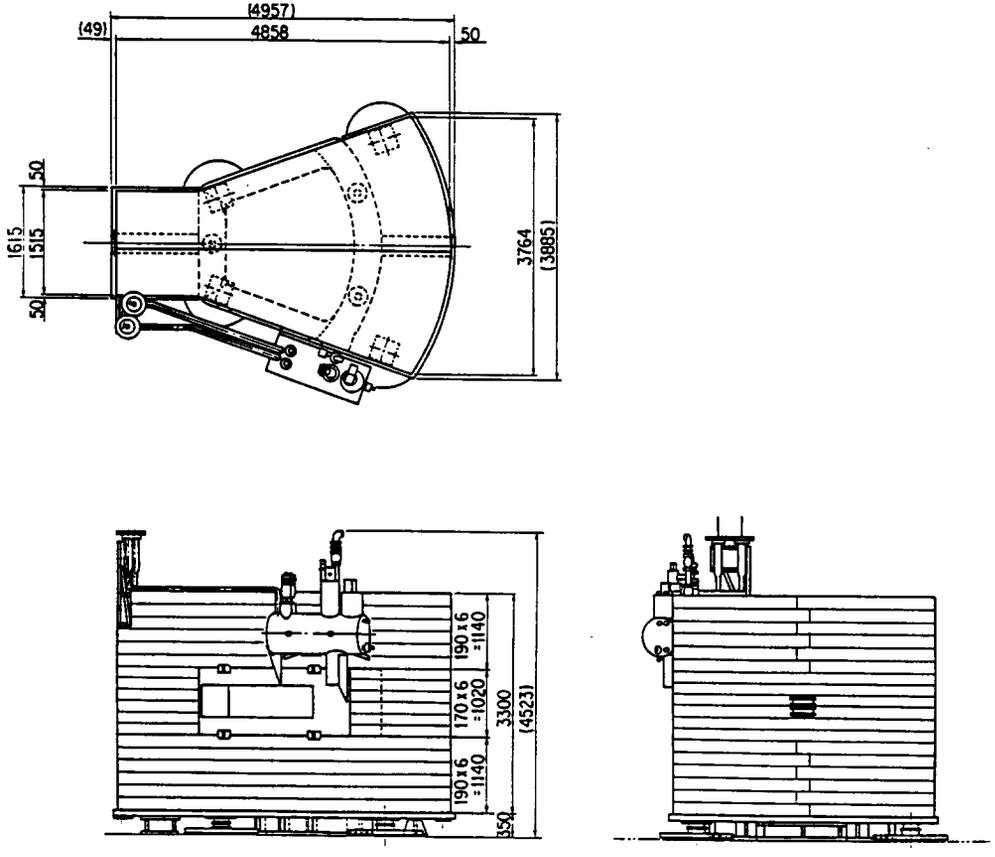

Figure 3: Schematic drawings of the SKS spectrometer magnet. The return yoke comprises 18 layers of iron plates.

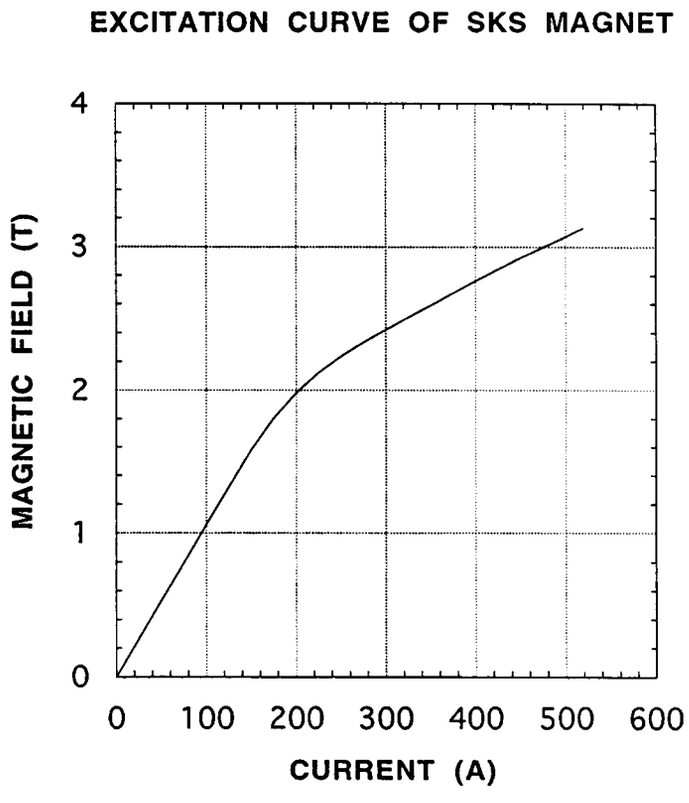

Figure 4: Excitation curve of the superconducting magnet.

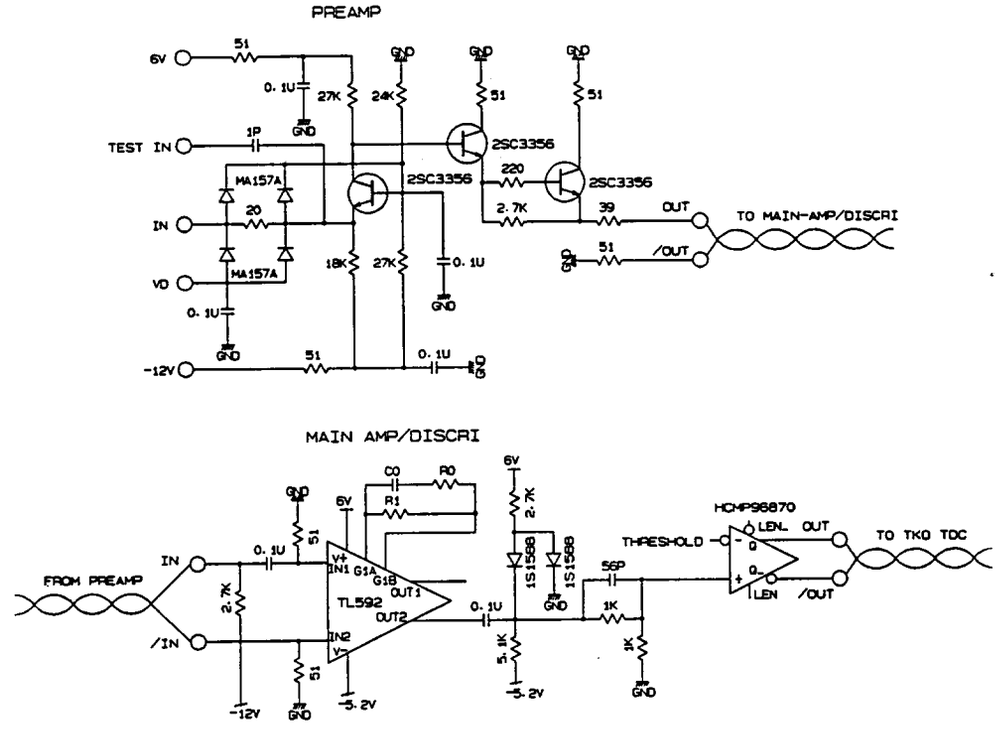

Figure 5: Schematic diagram of the preamplifier and the amplifier/discriminator module.

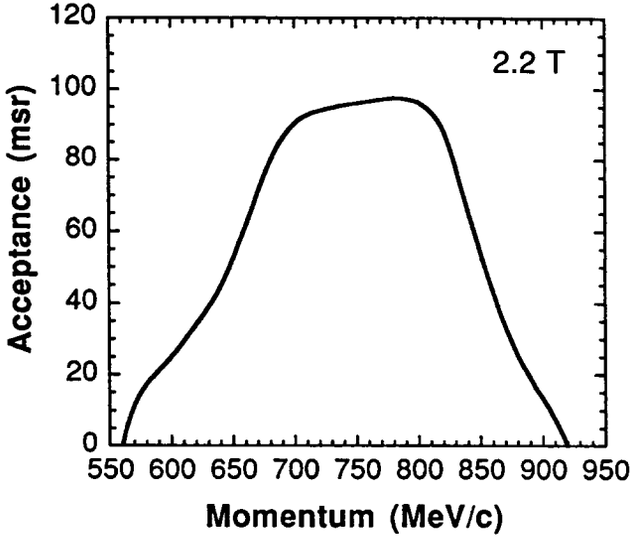

Figure 6: Acceptance of the SKS spectrometer for the (π^+,K^+) reaction as a function of the particle momentum.

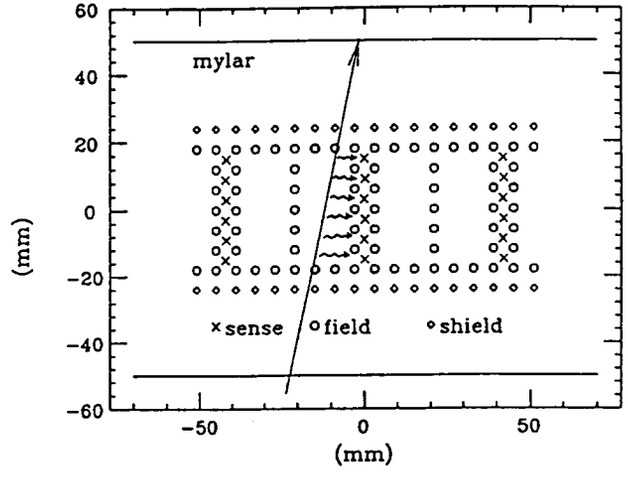

Figure 7: Drift-cell structure of SDC4. There are six anode planes in each cell with focusing wires. The anode wires are staggered by $\pm 200\mu$m.

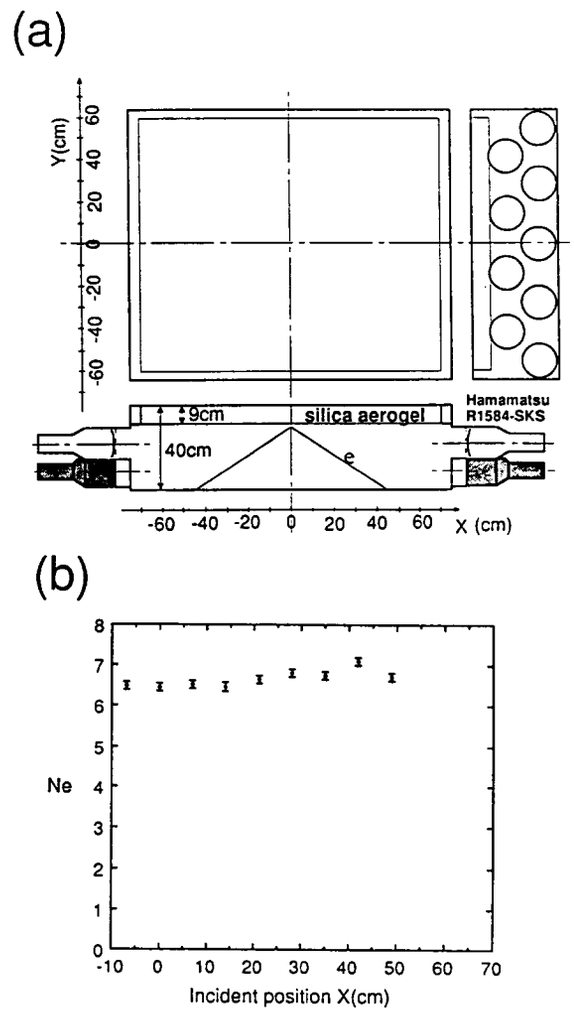

Figure 8: (a) Structure of the light diffusion box. (b) Position dependence of the number of photoelectrons obtained in one layer.

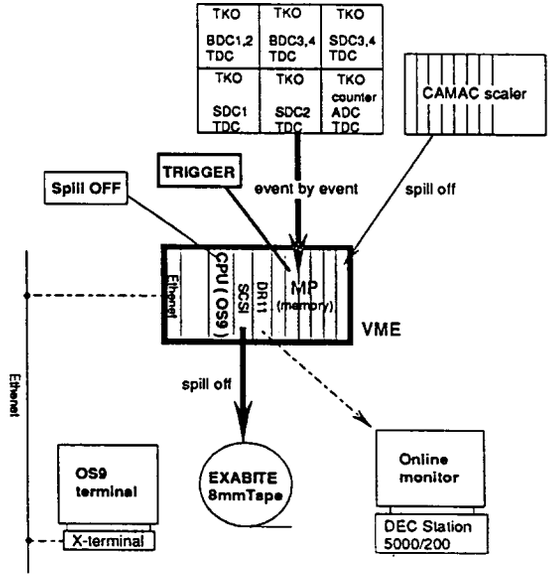

Figure 9: Diagram of the SKS data-taking system.

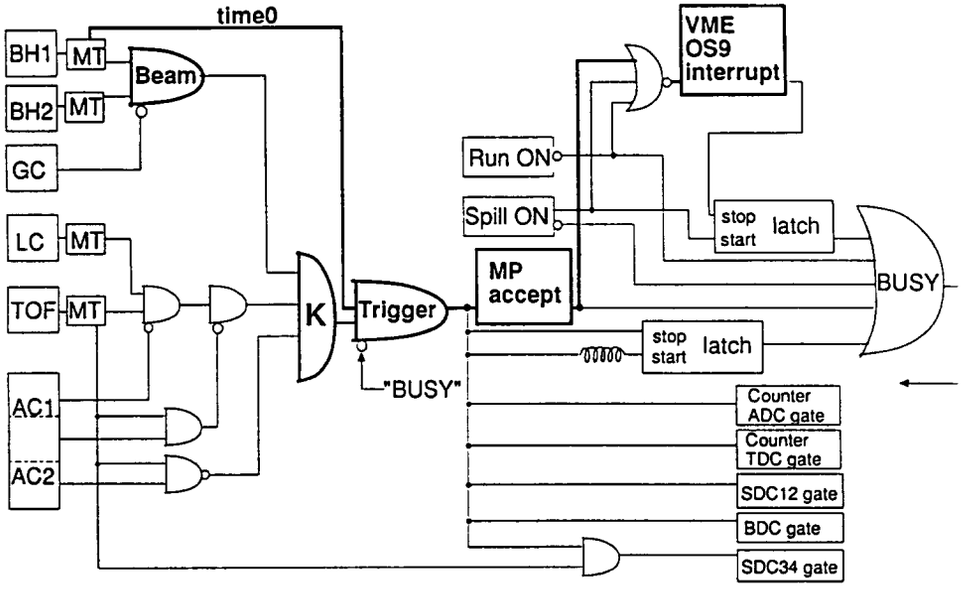

Figure 10: Logic diagram of the SKS for the (π^+,K^+) reaction.

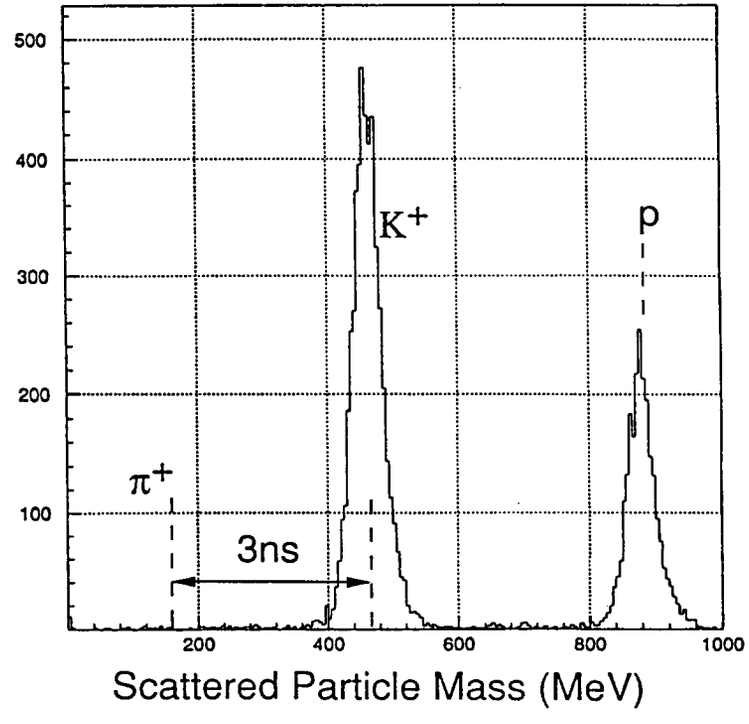

Figure 11: Mass distribution of the scattered particles based on TOF information and the momentum for the (π^+,K^+) reaction.

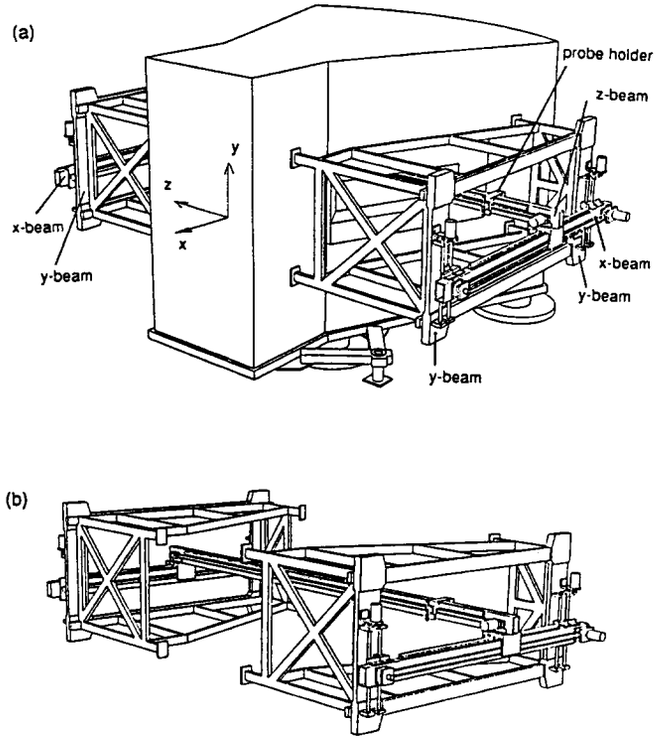

Figure 12: Bird's-eye view of the volume-scanning device for the magnetic-field measurement.

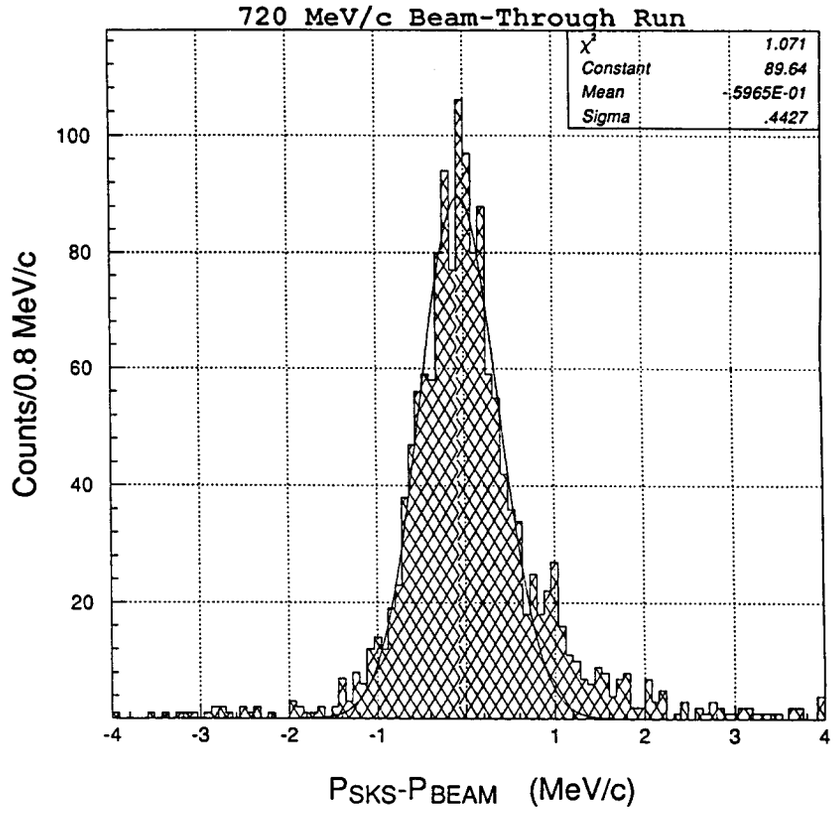

Figure 13: Difference in the momenta measured with the beam-line spectrometer and the SKS for a pion beam at 720 MeV/c. The width shows that the resolutions of the two spectrometers are 0.1%.

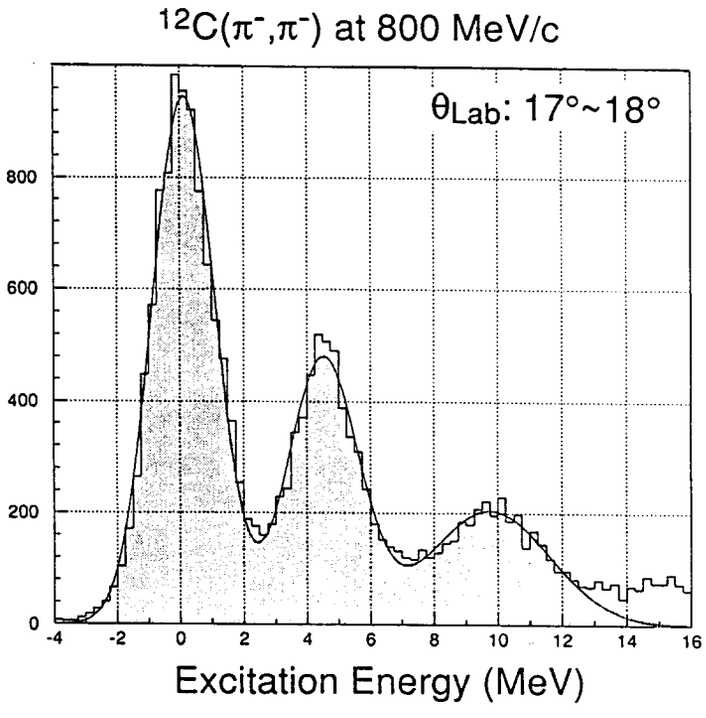

Figure 14: Excitation spectrum of ^{12}C in the reaction of 800 MeV/c π^- + ^{12}C.

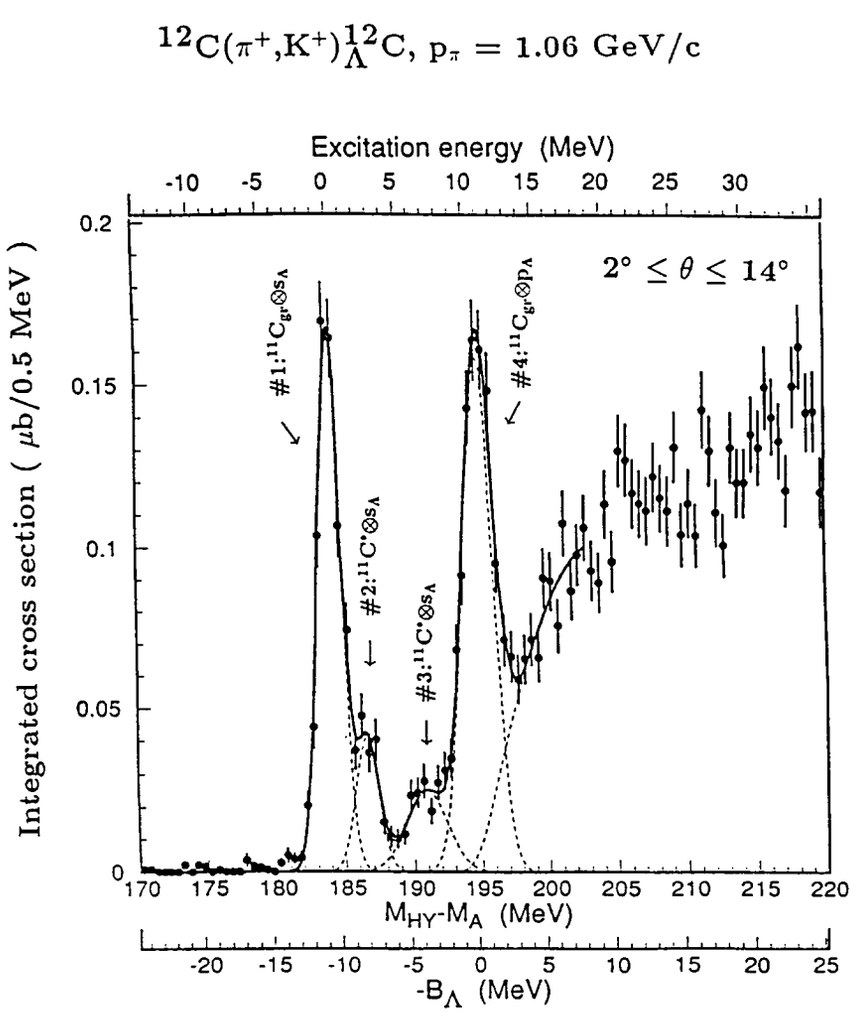

Figure 15: Hypernuclear spectrum measured by the reaction $^{12}C(\pi^+,K^+)^{12}_{\Lambda}C$ at 1.06 GeV/c.